Editors' Suggestion | Featured in Physics

Precision Measurement of Net-Proton-Number Fluctuations in Au + Au Collisions at RHIC

B. E. Aboona,[57] J. Adam,[17] L. Adamczyk,[3] I. Aggarwal,[44] M. M. Aggarwal,[44] Z. Ahammed,[65] A. K. Alshammri,[33] E. C. Aschenauer,[7] S. Aslam,[22] J. Atchison,[2] V. Bairathi,[55] X. Bao,[51] K. Barish,[12] S. Behera,[28] R. Bellwied,[25] P. Bhagat,[32] A. Bhasin,[32] S. Bhatta,[54] S. R. Bhosale,[3] J. Bielcik,[17] J. Bielcikova,[42] J. D. Brandenburg,[43] C. Broodo,[25] X. Z. Cai,[52] H. Caines,[69] M. Calderón de la Barca Sánchez,[10] D. Cebra,[10] J. Ceska,[17] I. Chakaberia,[36] P. Chaloupka,[17] B. K. Chan,[11] Z. Chang,[30] A. Chatterjee,[19] D. Chen,[12] J. Chen,[51] J. H. Chen,[22] Q. Chen,[23] Z. Chen,[51] J. Cheng,[60] Y. Cheng,[11] W. Christie,[7] X. Chu,[7] S. Corey,[43] H. J. Crawford,[9] M. Csanád,[20] G. Dale-Gau,[14] A. Das,[17] I. M. Deppner,[24] A. Deshpande,[54] A. Dhamija,[44] A. Dimri,[54] P. Dixit,[27] X. Dong,[36] J. L. Drachenberg,[2] E. Duckworth,[33] J. C. Dunlop,[7] J. Engelage,[9] G. Eppley,[46] S. Esumi,[61] O. Evdokimov,[14] O. Eyser,[7] R. Fatemi,[34] S. Fazio,[8] Y. Feng,[45] E. Finch,[53] Y. Fisyak,[7] F. A. Flor,[69] C. Fu,[31] T. Fu,[51] C. A. Gagliardi,[57] T. Galatyuk,[18] T. Gao,[51] F. Geurts,[46] N. Ghimire,[56] A. Gibson,[64] K. Gopal,[28] X. Gou,[51] D. Grosnick,[64] A. Gu,[26] A. Gupta,[32] W. Guryn,[7] A. Hamed,[5] R. J. Hamilton,[69] X. Han,[43] S. Harabasz,[18] M. D. Harasty,[10] J. W. Harris,[69] H. Harrison-Smith,[34] L. B. Havener,[69] X. H. He,[31] Y. He,[51] N. Herrmann,[24] L. Holub,[17] C. Hu,[62] Q. Hu,[31] Y. Hu,[36] H. Huang,[1,41] H. Z. Huang,[11] S. L. Huang,[54] T. Huang,[14] Y. Huang,[20] Y. Huang,[13] T. J. Humanic,[43] M. Isshiki,[61] W. W. Jacobs,[30] A. Jalotra,[32] C. Jena,[28] A. Jentsch,[7] Y. Ji,[36] J. Jia,[54,7] C. Jin,[46] N. Jindal,[43] X. Ju,[48] E. G. Judd,[9] S. Kabana,[55] D. Kalinkin,[34] K. Kang,[60] D. Kapukchyan,[12] K. Kauder,[7] D. Keane,[33] M. Kesler,[33] A. Khanal,[67] Y. V. Khyzhniak,[43] D. P. Kikoła,[66] J. Kim,[7] D. Kincses,[20] I. Kisel,[21] A. Kiselev,[7] A. G. Knospe,[37] J. Kołaś,[66] B. Korodi,[43] L. K. Kosarzewski,[43] L. Kumar,[44] M. C. Labonte,[10] R. Lacey,[54] J. M. Landgraf,[7] C. Larson,[34] J. Lauret,[7] A. Lebedev,[7] J. H. Lee,[7] Y. H. Leung,[24] C. Li,[13] D. Li,[48] H-S. Li,[45] H. Li,[68] H. Li,[23] W. Li,[46] X. Li,[48] X. Li,[48] Y. Li,[60] Z. Li,[49] Z. Li,[48] X. Liang,[12] Y. Liang,[33] R. Licenik,[42,17] T. Lin,[51] Y. Lin,[23] M. A. Lisa,[43] C. Liu,[31] G. Liu,[49] H. Liu,[26] L. Liu,[13] Z. Liu,[13] T. Ljubicic,[46] O. Lomicky,[17] R. S. Longacre,[7] E. M. Loyd,[12] T. Lu,[31] J. Luo,[48] X. F. Luo,[13] L. Ma,[22] R. Ma,[7] Y. G. Ma,[22] N. Magdy,[58] D. Mallick,[13] R. Manikandhan,[25] S. Margetis,[33] C. Markert,[59] O. Matonoha,[17] O. Mezhanska,[17] K. Mi,[13] S. Mioduszewski,[57] B. Mohanty,[40] B. Mondal,[40] M. M. Mondal,[40] I. Mooney,[69] J. Mrazkova,[42,17] M. I. Nagy,[20] C. J. Naim,[54] A. S. Nain,[44] J. D. Nam,[56] M. Nasim,[27] H. Nasrulloh,[48] D. Neff,[11] J. M. Nelson,[9] M. Nie,[51] G. Nigmatkulov,[14] T. Niida,[61] T. Nonaka,[61] G. Odyniec,[36] A. Ogawa,[7] S. Oh,[50] K. Okubo,[61] B. S. Page,[7] S. Pal,[17] A. Pandav,[36] A. Panday,[27] A. K. Pandey,[31] T. Pani,[47] A. Paul,[12] S. Paul,[54] D. Pawlowska,[66] C. Perkins,[9] J. Pluta,[66] B. R. Pokhrel,[56] I. D. Ponce Pinto,[69] M. Posik,[56] E. Pottebaum,[69] S. Prodhan,[28] T. L. Protzman,[37] A. Prozorov,[17] V. Prozorova,[17] N. K. Pruthi,[44] M. Przybycien,[3] J. Putschke,[67] Z. Qin,[60] H. Qiu,[31] C. Racz,[12] S. K. Radhakrishnan,[33] A. Rana,[44] R. L. Ray,[59] R. Reed,[37] C. W. Robertson,[45] M. Robotkova,[42,17] M. A. Rosales Aguilar,[34] D. Roy,[47] P. Roy Chowdhury,[66] L. Ruan,[7] A. K. Sahoo,[27] N. R. Sahoo,[28] H. Sako,[61] S. Salur,[47] S. S. Sambyal,[32] J. K. Sandhu,[37] S. Sato,[61] B. C. Schaefer,[37] N. Schmitz,[38] F-J. Seck,[18] J. Seger,[16] R. Seto,[12] P. Seyboth,[38] N. Shah,[29] P. V. Shanmuganathan,[7] T. Shao,[22] M. Sharma,[32] N. Sharma,[27] R. Sharma,[28] S. R. Sharma,[28] A. I. Sheikh,[33] D. Shen,[51] D. Y. Shen,[31] K. Shen,[48] S. Shi,[13] Y. Shi,[51] F. Si,[48] J. Singh,[55] S. Singha,[31] P. Sinha,[28] M. J. Skoby,[6,45] N. Smirnov,[69] Y. Söhngen,[24] Y. Song,[69] T. D. S. Stanislaus,[64] M. Stefaniak,[43] Y. Su,[48] M. Sumbera,[42] X. Sun,[31] Y. Sun,[48] B. Surrow,[56] M. Svoboda,[42,17] Z. W. Sweger,[10] A. C. Tamis,[69] A. H. Tang,[7] Z. Tang,[48] T. Tarnowsky,[39] J. H. Thomas,[36] A. R. Timmins,[25] D. Tlusty,[16] T. Todoroki,[61] D. Torres Valladares,[46] S. Trentalange,[11] P. Tribedy,[7] S. K. Tripathy,[66] T. Truhlar,[17] B. A. Trzeciak,[17] O. D. Tsai,[11,7] C. Y. Tsang,[33,7] Z. Tu,[7] J. Tyler,[57] T. Ullrich,[7] D. G. Underwood,[4,64] G. Van Buren,[7] J. Vanek,[7] I. Vassiliev,[21] F. Videbæk,[7] S. A. Voloshin,[67] F. Wang,[45] G. Wang,[11] J. S. Wang,[26] J. Wang,[51] K. Wang,[48] X. Wang,[51] Y. Wang,[48] Y. Wang,[13] Y. Wang,[60] Z. Wang,[51] A. J. Watroba,[3] J. C. Webb,[7] P. C. Weidenkaff,[24] G. D. Westfall,[39] D. Wielanek,[66] H. Wieman,[36] G. Wilks,[14] S. W. Wissink,[30] R. Witt,[63] C. P. Wong,[7] J. Wu,[13] J. Wu,[62] X. Wu,[11] Wu X.,[48] B. Xi,[22] Z. G. Xiao,[60] G. Xie,[62] W. Xie,[45] H. Xu,[26] N. Xu,[13] Q. H. Xu,[51] Y. Xu,[51] Y. Xu,[13] Z. Xu,[33] Z. Xu,[4] G. Yan,[51] Z. Yan,[54] C. Yang,[51] Q. Yang,[51] S. Yang,[49] Y. Yang,[1,41] Z. Ye,[49] Z. Ye,[36] L. Yi,[51] Y. Yu,[51] H. Zbroszczyk,[66] W. Zha,[48] C. Zhang,[22] D. Zhang,[49] J. Zhang,[51] S. Zhang,[15] W. Zhang,[49] X. Zhang,[31] Y. Zhang,[31] Y. Zhang,[48] Y. Zhang,[51] Y. Zhang,[23] Z. Zhang,[7] Z. Zhang,[14] F. Zhao,[35] J. Zhao,[22] M. Zhao,[7] S. Zhou,[13] Y. Zhou,[13] X. Zhu,[60] M. Zurek,[4,7] and M. Zyzak[21]

(STAR Collaboration)

[1]*Academia Sinica, Taipei 115201*
[2]*Abilene Christian University, Abilene, Texas 79699*

 © 2025 American Physical Society

[3]AGH University of Krakow, FPACS, Cracow 30-059, Poland
[4]Argonne National Laboratory, Argonne, Illinois 60439
[5]American University in Cairo, New Cairo 11835, Egypt
[6]Ball State University, Muncie, Indiana 47306
[7]Brookhaven National Laboratory, Upton, New York 11973
[8]University of Calabria and INFN-Cosenza, Rende 87036, Italy
[9]University of California, Berkeley, California 94720
[10]University of California, Davis, California 95616
[11]University of California, Los Angeles, California 90095
[12]University of California, Riverside, California 92521
[13]Central China Normal University, Wuhan, Hubei 430079
[14]University of Illinois at Chicago, Chicago, Illinois 60607
[15]Chongqing University, Chongqing, 401331
[16]Creighton University, Omaha, Nebraska 68178
[17]Czech Technical University in Prague, FNSPE, Prague 115 19, Czech Republic
[18]Technische Universität Darmstadt, Darmstadt 64289, Germany
[19]National Institute of Technology Durgapur, Durgapur 713209, India
[20]ELTE Eötvös Loránd University, Budapest, Hungary H-1117
[21]Frankfurt Institute for Advanced Studies FIAS, Frankfurt 60438, Germany
[22]Fudan University, Shanghai, 200433
[23]Guangxi Normal University, Guilin, 541004
[24]University of Heidelberg, Heidelberg 69120, Germany
[25]University of Houston, Houston, Texas 77204
[26]Huzhou University, Huzhou, Zhejiang 313000
[27]Indian Institute of Science Education and Research (IISER), Berhampur 760010, India
[28]Indian Institute of Science Education and Research (IISER) Tirupati, Tirupati 517507, India
[29]Indian Institute Technology, Patna, Bihar 801106, India
[30]Indiana University, Bloomington, Indiana 47408
[31]Institute of Modern Physics, Chinese Academy of Sciences, Lanzhou, Gansu 730000
[32]University of Jammu, Jammu 180001, India
[33]Kent State University, Kent, Ohio 44242
[34]University of Kentucky, Lexington, Kentucky 40506-0055
[35]Lanzhou University, Lanzhou 730000
[36]Lawrence Berkeley National Laboratory, Berkeley, California 94720
[37]Lehigh University, Bethlehem, Pennsylvania 18015
[38]Max-Planck-Institut für Physik, Munich 80805, Germany
[39]Michigan State University, East Lansing, Michigan 48824
[40]National Institute of Science Education and Research, HBNI, Jatni 752050, India
[41]National Cheng Kung University, Tainan 70101
[42]Nuclear Physics Institute of the CAS, Rez 250 68, Czech Republic
[43]The Ohio State University, Columbus, Ohio 43210
[44]Panjab University, Chandigarh 160014, India
[45]Purdue University, West Lafayette, Indiana 47907
[46]Rice University, Houston, Texas 77251
[47]Rutgers University, Piscataway, New Jersey 08854
[48]University of Science and Technology of China, Hefei, Anhui 230026
[49]South China Normal University, Guangzhou, Guangdong 510631
[50]Sejong University, Seoul, 05006, South Korea
[51]Shandong University, Qingdao, Shandong 266237
[52]Shanghai Institute of Applied Physics, Chinese Academy of Sciences, Shanghai 201800
[53]Southern Connecticut State University, New Haven, Connecticut 06515
[54]State University of New York, Stony Brook, New York 11794
[55]Instituto de Alta Investigación, Universidad de Tarapacá, Arica 1000000, Chile
[56]Temple University, Philadelphia, Pennsylvania 19122
[57]Texas A&M University, College Station, Texas 77843
[58]Texas Southern University, Houston, Texas 77004
[59]University of Texas, Austin, Texas 78712
[60]Tsinghua University, Beijing 100084
[61]University of Tsukuba, Tsukuba, Ibaraki 305-8571, Japan
[62]University of Chinese Academy of Sciences, Beijing 101408

[63]United States Naval Academy, Annapolis, Maryland 21402
[64]Valparaiso University, Valparaiso, Indiana 46383
[65]Variable Energy Cyclotron Centre, Kolkata 700064, India
[66]Warsaw University of Technology, Warsaw 00-661, Poland
[67]Wayne State University, Detroit, Michigan 48201
[68]Wuhan University of Science and Technology, Wuhan, Hubei 430065
[69]Yale University, New Haven, Connecticut 06520

(Received 26 March 2025; accepted 18 July 2025; published 29 September 2025)

We report precision measurements on cumulants (C_n) and factorial cumulants (κ_n) of (net) proton number distributions up to fourth order in Au + Au collisions over center-of-mass energies $\sqrt{s_{NN}} =$ 7.7–27 GeV from phase II of the Beam Energy Scan program at RHIC. (Anti)protons are selected at midrapidity ($|y| < 0.5$) within a transverse momentum range of $0.4 < p_T < 2.0$ GeV/c. Relative to various noncritical-point model calculations and peripheral collision 70%–80% data, the net proton C_4/C_2 measurement in 0%–5% collisions shows a minimum around 19.6 GeV for significance of deviation at ~2–5σ. A minimum in C_4/C_2 with respect to a noncritical baseline is expected to be a characteristic feature of the signature associated with a critical point in the QCD phase diagram. In addition, deviations from noncritical baselines around the same collision energy region are also seen in proton factorial cumulant ratios, especially in κ_2/κ_1 and κ_3/κ_1. Dynamical model calculations including a critical point are called for in order to understand these precision measurements.

DOI: 10.1103/9l69-2d7p

A key focus of experiments involving the collision of heavy ions at high energy has long been the search for a possible critical point associated with the phase transitions of matter interacting via the strong force. In the phase diagram of such matter, known as the quantum chromodynamics (QCD) phase diagram, the critical point marks the boundary between a crossover quark-hadron transition at low baryochemical potential (μ_B) and a possible first-order transition at higher μ_B [1–3]. While first-principle calculations based on lattice QCD have established the crossover at small μ_B [4], the extension of theoretical methods to enable calculations at large μ_B remains a challenge. Extensive efforts are underway to search for a possible critical point in the QCD phase diagram.

Fluctuations of event-by-event net proton number in nuclear collision experiments have been suggested as sensitive probes to search for the QCD critical point (CP) [5–7]. The fluctuations of a variable are often quantified via cumulants. Cumulants of net proton number (N) up to fourth order can be expressed as $C_1 = \langle N \rangle$, $C_2 = \langle \delta N^2 \rangle$, $C_3 = \langle \delta N^3 \rangle$, and $C_4 = \langle \delta N^4 \rangle - 3\langle \delta N^2 \rangle$, where $\delta N = N - \langle N \rangle$. These cumulants are related to the correlation length (ξ) of the system formed in heavy-ion collisions [7], which diverges at a critical point. Ratios of cumulants can be related to ratios of thermodynamic number susceptibilities obtained in various theory calculations [8–11]. A nonmonotonic dependence on collision energy in the ratio of the fourth- to the second-order net proton cumulant (C_4/C_2, also often referred to as the moment product $\kappa\sigma^2$, where κ is the kurtosis and σ^2 is the variance [12]) relative to baseline fluctuations has been proposed by a model-based study as the signature of the CP [7]. In the first phase of the Beam Energy Scan (BES-I) program at RHIC, the Solenoidal Tracker at RHIC (STAR) experiment extensively analyzed net proton fluctuations [12–17]. However, precision measurements were needed to reduce the large uncertainties on the first set of results [15] to draw concrete conclusions. Recent C_4/C_2 results from STAR's fixed target (FXT) Au + Au collisions at $\sqrt{s_{NN}} = 3$ GeV show suppressed values relative to higher collision energies and are consistent with a hadronic transport model without a CP [18,19]. A second phase of the Beam Energy Scan (BES-II) with large event statistics at $\sqrt{s_{NN}} =$ 7.7–27 GeV and important detector upgrades, including the replacement of the inner sectors of the Time Projection Chamber (iTPC) [20], has recently been concluded.

This Letter presents the latest results on net proton cumulants up to fourth order from Au + Au collisions at $\sqrt{s_{NN}} = 7.7$, 9.2, 11.5, 14.6, 17.3, 19.6, and 27 GeV from the BES-II program. All datasets were taken in collider mode. The two energies $\sqrt{s_{NN}} = 9.2$ and 17.3 GeV were not present in BES-I. Furthermore, proton factorial cumulants (κ_n), also suggested as promising probes for CP search [21,22], are reported up to the fourth order. They are defined as $\kappa_1 = C_1, \kappa_2 = -C_1 + C_2, \kappa_3 = 2C_1 - 3C_2 + C_3$, and $\kappa_4 = -6C_1 + 11C_2 - 6C_3 + C_4$. The factorial cumulant of a certain order reflects genuine multiparticle correlation of that order, whereas the regular cumulant of that order also contains contributions from lower orders.

TABLE I. Total event statistics (at 10^6) in Au + Au collisions for various collision energies ($\sqrt{s_{NN}}$) in BES-II.

$\sqrt{s_{NN}}$ (GeV)	7.7	9.2	11.5	14.6	17.3	19.6	27
Events (10^6)	45	78	116	178	116	270	220

Au + Au collisions resulting in signals in the trigger detectors above the noise threshold level (minimum bias) are analyzed [23,24]. The z coordinate of the interaction point (also called the primary vertex) is denoted V_z and is constrained to be within ± 50 cm from the center of the STAR detector at all energies except 27 GeV, where it is ± 27 cm to ensure uniform acceptance and efficiency of the TPC. This choice of V_z cut at $\sqrt{s_{NN}} = 27$ GeV is due to reduced TPC acceptance as the iTPC upgrade had not taken place by the time of data taking. The total numbers of analyzed events are listed in Table I and are about 7–18 times larger than available in BES-I [12]. (Anti)protons are identified within a rapidity acceptance of $|y| < 0.5$ and transverse momentum range of $p_T = 0.4$–2.0 GeV/c based on their ionization energy loss using the TPC. Along with the TPC, the time-of-flight detector is used from $p_T = 0.8$–2.0 GeV/c [25]. This ensures a high purity, ~99% over the full y–p_T phase space. The distance of the closest approach (DCA) of a track to the primary vertex is taken to be less than 1 cm to suppress contributions from secondaries [14] and weak decays [26]. Moreover, the weak decays only mildly affect the cumulant ratios [27,28].

Figure 1(a) presents the $y - p_T$ acceptance of (anti) proton yields identified by the TPC in Au + Au collisions at $\sqrt{s_{NN}} = 19.6$ GeV from BES-I (smaller band) and BES-II (larger band). The acceptance for the current analysis ($|y| < 0.5$ and $0.4 < p_T < 2.0$ GeV/c) is the same as that used in BES-I [15] [shown as a dashed box in Fig. 1(a)]. The iTPC upgrade in BES-II highly extends the acceptance, which provides a possibility of measurement over $|y| < 0.7$ in the future. Figure 1(b) shows the reference charged particle multiplicity distributions from data: RefMult3 and RefMult3X used for defining collision centrality. They are defined by the charged particle multiplicities, not corrected for efficiency, within $|\eta| < 1.0$ and $|\eta| < 1.6$, respectively, after excluding protons and antiprotons to avoid the self-correlation effect [29,30]. Because of the increased efficiency from the iTPC, RefMult3 is larger in BES-II than it was in BES-I. RefMult3X is larger still, due to the larger η acceptance. Larger multiplicity ranges lead to better centrality resolution. The RefMult3 and RefMult3X distributions are fitted with multiplicity obtained from a Glauber model simulation to extract the number of participating nucleons ($N_{\rm part}$) and determine the centrality cuts. An event-weighted averaging called the centrality-bin-width correction (CBWC) was performed on the measurements for a given centrality [31] (see Fig. 1 of

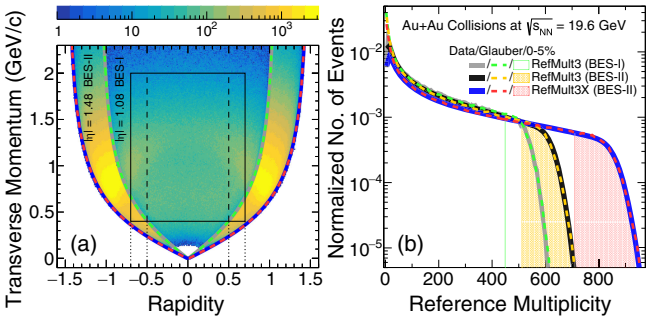


FIG. 1. (a) (Anti)proton acceptances from the TPC in transverse momentum (p_T) vs rapidity (y) phase space in Au + Au collisions at $\sqrt{s_{NN}} = 19.6$ GeV from BES-II and BES-I. The green and red dashed curves describe the pseudorapidity (η) boundaries of the acceptances in BES-I ($|\eta| = 1.08$) and BES-II ($|\eta| = 1.48$), respectively. Only BES-I acceptance is plotted in the common region. (Anti)protons are selected in the 0%–5% most central events within $13 < V_z < 15$ cm for positive rapidities and $-15 < V_z < -13$ cm for negative rapidities. These V_z ranges are taken just as an example. The dashed box denotes the acceptance criterion ($|y| < 0.5$) for this analysis, which is the same as BES-I. (b) Reference charged particle multiplicity distributions RefMult3 (BES-I green line and BES-II black line) and RefMult3X (BES-II blue line). Distributions from data and Glauber fits are presented. The shaded bands reflect the 0%–5% central collision events.

the Supplemental Material for details [32]). The measurements are corrected for finite detector efficiency by assuming the detector response to be binomial [33–37]. The track selection cuts, background estimates, and detector efficiency are varied for evaluating systematic uncertainties on the measurements. All sources of systematics are subjected to a Barlow check [38] and are added in quadrature to obtain total systematic uncertainties ($\sigma_{\rm sys}$). For net proton C_4/C_2 measurements, the particle identification (PID) and DCA variations are dominant contributors. As an example, at $\sqrt{s_{NN}} = 7.7$ GeV, PID and DCA contribution are 88% and 47% of $\sigma_{\rm sys}$ for 0%–5% centrality, respectively. Enhanced event statistics and better tracking and PID from iTPC in BES-II lead to a significant reduction of uncertainties. A factor of 4.7 (3.2) reduction in statistical (systematic) uncertainties on net proton C_4/C_2 in the central collisions from BES-II has been achieved compared to that in BES-I.

Net proton cumulants (C_n) up to fourth order from BES-II as a function of collision centrality are shown in Fig. 2 along with those from BES-I. In general, the cumulants smoothly increase as a function of centrality and decrease from lower to higher collision energies. Higher-order cumulants measured using RefMult3X for centrality are lower than those using RefMult3, and those using RefMult3 in BES-II are lower than those seen in BES-I, though mostly consistent within uncertainties. Such a trend is expected due to the differences in centrality

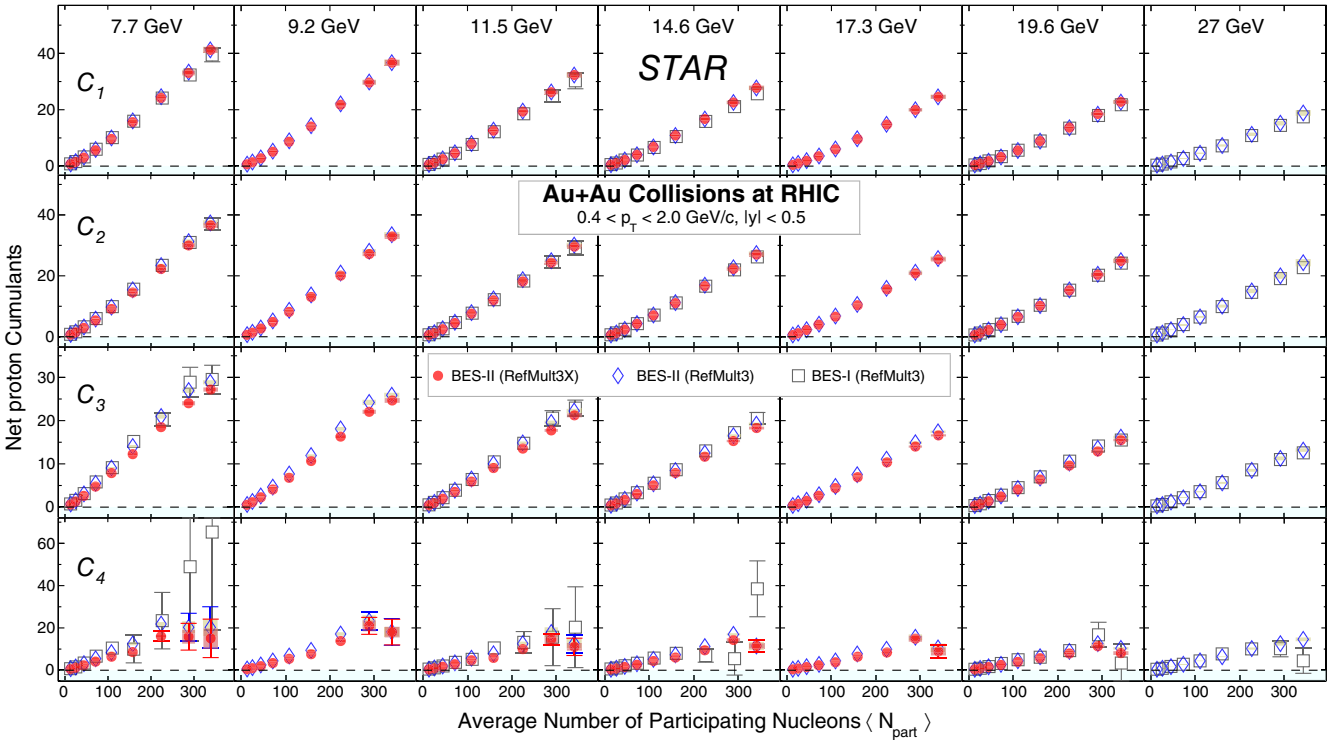


FIG. 2. Cumulants of net proton multiplicity distribution from $\sqrt{s_{NN}} = 7.7$–27 GeV as a function of collision centrality ($\langle N_{\rm part}\rangle$; average number of participating nucleons) in Au + Au collisions. (Anti)protons are measured at midrapidity ($|y| < 0.5$) within $0.4 < p_T < 2.0$ GeV/c. Results from BES-II with RefMult3X (RefMult3) used for centrality definition are shown as red (blue) markers, while those from BES-I [12,15] (RefMult3) are shown as open squares. The bars and bands on the data points from BES-II represent statistical and systematic uncertainties, respectively. Total uncertainties are shown for BES-I data points as bars on data points.

resolution [31] (see Supplemental Material for more discussion [32]). Factorial cumulants, being a combination of regular cumulants, also show such dependence on resolution. Note that, due to the absence of the iTPC during recording of $\sqrt{s_{NN}} = 27$ GeV Au + Au collisions from BES-II, only results using RefMult3 are presented at this energy. C_4 measurements as well as the cumulant ratio C_4/C_2 in 0%–5% collisions are consistent across different centrality measures and are consistent with BES-I data (see Fig. 4 of Supplemental Material for details [32]).

Figure 3 shows the collision energy dependence of ratios of net proton cumulants and proton factorial cumulants from BES-II and BES-I for the most central 0%–5% and peripheral 70%–80% collisions. BES-II results shown are measured with RefMult3X for centrality definition except for $\sqrt{s_{NN}} = 27$ GeV. By construction, the Poisson baseline for net proton cumulant ratios is at unity, while for proton factorial cumulants it is at zero. A strong deviation from the Poisson baseline is observed in all ratios. The cumulant ratios for 0%–5% centrality decrease with decreasing collision energy except at low energies where hint of a possible rise can be seen, albeit with significant uncertainties. As mentioned earlier, the factorial cumulants reflect genuine multiparticle correlation. In the case of proton κ_2/κ_1 and κ_4/κ_1, for 0%–5% central collisions, a similar trend in collision energy dependence is observed as seen for the net proton cumulant ratios in the same collision centrality. For κ_3/κ_1 (0%–5%), from high to low collision energy, an initial increase followed by a dip toward the Poisson baseline is observed. The peripheral 70%–80% collision data are closer to the Poisson baseline at zero compared to 0%–5% data and for κ_4/κ_1 it is consistent with zero at all energies.

The data are compared to three theoretical models that do not include a critical point. The first is the hadronic transport model UrQMD [40,41], a microscopic approach that incorporates nonequilibrium dynamics and hadronic scatterings, but lacks a quark-gluon plasma (QGP) phase. The second is the thermal model HRG CE [39], which is a statistical model describing a gas of hadrons in thermal equilibrium with a canonical treatment of baryon charge. The third is a hydrodynamic model with excluded volume effects (Hydro EV) [27], which simulates the space-time evolution of the medium under the assumption of local thermal equilibrium and accounts for repulsive interactions among hadrons through excluded volume corrections applied after particlization. These are distinct theoretical models describing the dynamics of QGP evolution and all of them incorporate exact baryon number conservation, an important aspect to be considered, especially at low

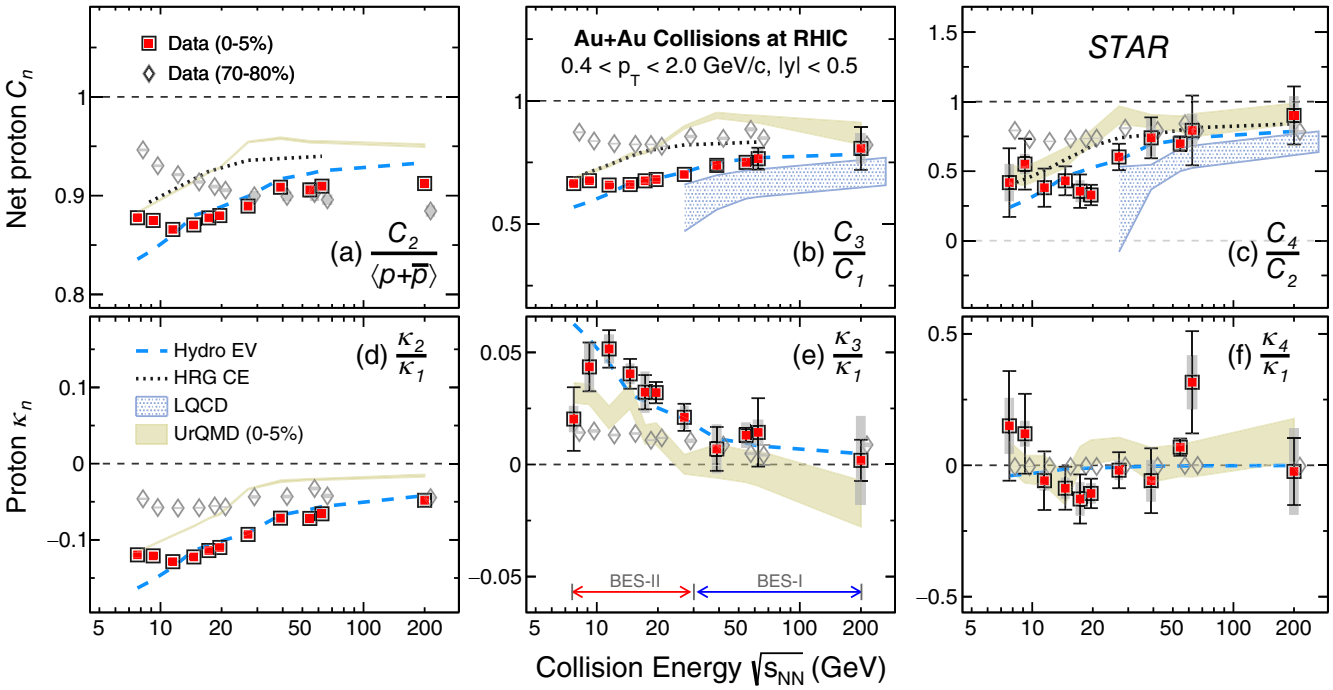


FIG. 3. Net proton cumulant ratios: (a) $C_2/\langle p+\bar{p}\rangle$, (b) C_3/C_1, and (c) C_4/C_2 and proton factorial cumulant ratios: (d) κ_2/κ_1, (e) κ_3/κ_1, and (f) κ_4/κ_1 in Au + Au collisions. Results from BES-II ($\sqrt{s_{NN}} = 7.7$–19.6 GeV with RefMult3X, 27 GeV with RefMult3) and BES-I [12,15] ($\sqrt{s_{NN}} = 39$–200 GeV with RefMult3) program at RHIC are shown. (Anti)protons are measured at midrapidity ($|y| < 0.5$) within $0.4 < p_T < 2.0$ GeV/c. The bars and bands on the data points reflect statistical and systematic uncertainties, respectively. Theoretical calculations from a hydrodynamical model [27] (blue dashed line), thermal model with canonical treatment for baryon charge [39] (black dashed line), transport model [40,41] (UrQMD, brown band), and lattice QCD [42,43] (light blue band, for net-baryon fluctuations) are also presented.

collision energies. The UrQMD results are analyzed in the same way as the experimental data. None of the models fully describe the collision energy dependence of the data. Based on BES-I, possible evidence of a nonmonotonic trend in 0%–5% C_4/C_2 with respect to the Poisson baseline was reported [15]. However, the precision data from BES-II do not support such a trend and always remain below the Poisson baseline. The new data, although closer to the noncritical model calculations with baryon number conservation than to Poisson expectations, exhibit a deviation from the former at around 20 GeV (see more discussion in Fig. 4).

STAR has previously reported proton C_4/C_2 measurement at $\sqrt{s_{NN}} = 3$ GeV with the rapidity acceptance of $-0.5 < y < 0$ from its FXT program [18,19]. Good agreement between data and UrQMD had been observed. In addition, data for $\sqrt{s_{NN}} > 27$ GeV are found to be consistent with these non-CP model calculations and lattice-QCD (LQCD) calculations with grand canonical ensemble [42]. LQCD studies indicate no sign of a critical point corresponding to chemical freeze-out points (μ_B, T) for $\sqrt{s_{NN}} > 27$ GeV and instead suggest a crossover in this regime.

The deviation between experimental data and noncritical baselines and references is shown in Fig. 4 for net proton C_4/C_2 (a), proton κ_2/κ_1 (b), proton κ_3/κ_1 (c), and proton

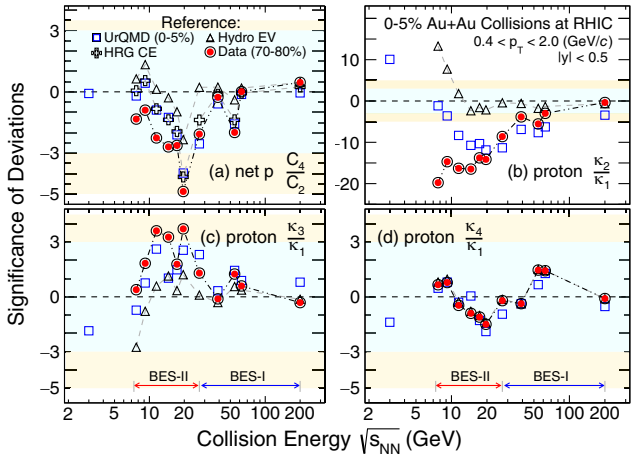


FIG. 4. Significance of deviation (data-reference)/σ_{total} for (a) net proton cumulant ratios C_4/C_2; proton factorial cumulant ratios (b) κ_4/κ_1; (c) κ_3/κ_1, and (d) κ_2/κ_1 in 0%–5% Au + Au collisions [12,15,18,19]. References include the noncritical model calculations, such as the UrQMD transport model [40,41] (blue square), HRG with canonical ensemble for baryon charge [39] (black cross), hydrodynamic model with excluded volume [27] (black triangle), and data from 70%–80% peripheral collisions (red dots).

κ_4/κ_1 (d). These deviations are obtained by taking the difference between the 0%–5% data and baselines and dividing with the total uncertainties (σ_{total}, obtained adding uncertainties in data and baselines in quadrature). Three typical calculations including the UrQMD, the HRG CE, and the hydro EV are used in the analysis. In addition, the 70%–80% peripheral collision data are used for comparison.

For the net proton cumulant ratio C_4/C_2, maximum negative deviations of 2–5σ are seen at $\sqrt{s_{NN}} = 19.6$ GeV from all references. The 5σ (2σ) significance corresponds to the case of using peripheral data (hydro EV calculations) as a reference. A minimum at same collision energy is also seen for data after subtracting the references (see Fig. 5 of the Supplemental Material [32]). This is particularly notable, as the deviation from the baseline is expected to be universally negative when the critical point is approached from the crossover side of the phase separation line [7]. On the other hand, in the case of collisions at 3 GeV [18] or above 27 GeV [15], the central data are consistent with all of the references within ~2σ. For the factorial cumulant ratios, the significance of the deviation decreases as a function of the order of the correlation: the maximum deviation is seen in κ_2/κ_1, while the minimum is in κ_4/κ_1, shown in Figs. 4(b) and 4(d), respectively. Clearly, precise experimental data between $\sqrt{s_{NN}} = 3.0$ and 7.7 GeV are needed to extend the search for the signal of the QCD critical point and the first-order phase boundary at the high baryon density region. The exploration of this region with precision measurements is currently underway using STAR's FXT program. Dynamical models that incorporate a critical point and simulate the system's evolution are needed for a quantitative interpretation of the measurements [44].

In summary, new high precision data on net proton cumulants and proton factorial cumulants and their ratios from the second phase of RHIC beam energy scan ($\sqrt{s_{NN}} = 7.7$–27 GeV, corresponding to $\mu_B =$ 400–150 MeV [45]) are reported in this Letter. Along with improved statistics, the RHIC BES-II program provides better centrality resolution and better control on the systematic uncertainties of the measurements. New net proton C_4/C_2 data in 0%–5% Au + Au collisions are consistent with those from BES-I. They remain below the Poisson baseline at unity at all collision energies. The new results compared to noncritical model calculations and peripheral 70%–80% data show a minimum for significance of deviation around 19.6 GeV at ~2–5σ. The highest (lowest) significance level of 5σ (2σ) deviation corresponds to the case of peripheral collision data (hydro EV calculations) taken as the baseline. Deviations are also seen for proton factorial cumulant ratios, with higher significance for κ_2/κ_1 and κ_3/κ_1 compared to κ_4/κ_1. As it has been argued [7], a minimum in net proton C_4/C_2 data with respect to the noncritical baseline is a characteristic feature of the proposed signature of a critical point in the QCD phase diagram. Dynamical model calculations including the criticality are needed to fully understand the data. These data will be crucial for constraining the equation of state [44] of the medium created in these collisions.

Acknowledgments—We thank the RHIC Operations Group and SDCC at BNL, the NERSC Center at LBNL, and the Open Science Grid consortium for providing resources and support. This work was supported in part by the Office of Nuclear Physics within the U.S. DOE Office of Science, the U.S. National Science Foundation, the Ministry of Science and Technology of China and the Chinese Ministry of Education, National Natural Science Foundation of China, Chinese Academy of Science, NSTC Taipei, the National Research Foundation of Korea, Czech Science Foundation and Ministry of Education, Youth and Sports of the Czech Republic, Hungarian National Research, Development and Innovation Office, New National Excellency Programme of the Hungarian Ministry of Human Capacities, Department of Atomic Energy and Department of Science and Technology of the Government of India, the National Science Centre and WUT ID-UB of Poland, the Ministry of Science, Education and Sports of the Republic of Croatia, German Bundesministerium für Bildung, Wissenschaft, Forschung and Technologie (BMBF), Helmholtz Association, Ministry of Education, Culture, Sports, Science, and Technology (MEXT), and Japan Society for the Promotion of Science (JSPS).

Data availability—The data that support the findings of this Letter are openly available [46].

[1] K. Rajagopal and F. Wilczek, The condensed matter physics of QCD, in *At the Frontier of Particle Physics. Handbook of QCD. Vol. 1-3*, edited by M. Shifman and B. Ioffe (World Scientific Publishing Co., Singapore, 2000), pp. 2061–2151.
[2] A. Bzdak, S. Esumi, V. Koch, J. Liao, M. Stephanov, and N. Xu, Phys. Rep. **853**, 1 (2020).
[3] A. Pandav, D. Mallick, and B. Mohanty, Prog. Part. Nucl. Phys. **125**, 103960 (2022).
[4] Y. Aoki, G. Endrodi, Z. Fodor, S. D. Katz, and K. K. Szabo, Nature (London) **443**, 675 (2006).
[5] M. A. Stephanov, Phys. Rev. Lett. **102**, 032301 (2009).
[6] M. Asakawa, S. Ejiri, and M. Kitazawa, Phys. Rev. Lett. **103**, 262301 (2009).
[7] M. A. Stephanov, Phys. Rev. Lett. **107**, 052301 (2011).
[8] R. V. Gavai and S. Gupta, Phys. Lett. B **696**, 459 (2011).
[9] S. Gupta, X. Luo, B. Mohanty, H. G. Ritter, and N. Xu, Science **332**, 1525 (2011).
[10] F. Karsch and K. Redlich, Phys. Lett. B **695**, 136 (2011).
[11] P. Garg, D. K. Mishra, P. K. Netrakanti, B. Mohanty, A. K. Mohanty, B. K. Singh, and N. Xu, Phys. Lett. B **726**, 691 (2013).

[12] M. Abdallah *et al.* (STAR Collaboration), Phys. Rev. C **104**, 024902 (2021); **111**, 029902(E) (2025).
[13] M. M. Aggarwal *et al.* (STAR Collaboration), Phys. Rev. Lett. **105**, 022302 (2010).
[14] L. Adamczyk *et al.* (STAR Collaboration), Phys. Rev. Lett. **112**, 032302 (2014).
[15] J. Adam *et al.* (STAR Collaboration), Phys. Rev. Lett. **126**, 092301 (2021); **134**, 139902(E) (2025).
[16] M. Abdallah *et al.* (STAR Collaboration), Phys. Rev. Lett. **127**, 262301 (2021); **134**, 139903(E) (2025).
[17] B. Aboona *et al.* (STAR Collaboration), Phys. Rev. Lett. **130**, 082301 (2023); **134**, 139901(E) (2025).
[18] M. S. Abdallah *et al.* (STAR Collaboration), Phys. Rev. Lett. **128**, 202303 (2022).
[19] M. Abdallah *et al.* (STAR Collaboration), Phys. Rev. C **107**, 024908 (2023).
[20] STAR Collaboration, Technical Design Report for the iTPC Upgrade, STAR Note SN0644, 2015, https://drupal.star.bnl.gov/STAR/starnotes/public/sn0644.
[21] B. Ling and M. A. Stephanov, Phys. Rev. C **93**, 034915 (2016).
[22] A. Bzdak, V. Koch, and N. Strodthoff, Phys. Rev. C **95**, 054906 (2017).
[23] C. Adler, A. Denisov, E. Garcia, M. J. Murray, H. Strobele, and S. N. White, Nucl. Instrum. Methods Phys. Res., Sect. A **470**, 488 (2001).
[24] W. J. Llope *et al.*, Nucl. Instrum. Methods Phys. Res., Sect. A **522**, 252 (2004).
[25] K. H. Ackermann *et al.* (STAR Collaboration), Nucl. Instrum. Methods Phys. Res., Sect. A **499**, 624 (2003).
[26] C. Adler *et al.* (STAR Collaboration), Phys. Rev. Lett. **86**, 4778 (2001); **90**, 119903(E) (2003).
[27] V. Vovchenko, V. Koch, and C. Shen, Phys. Rev. C **105**, 014904 (2022).
[28] Y. Zhang, S. He, H. Liu, Z. Yang, and X. Luo, Phys. Rev. C **101**, 034909 (2020).
[29] A. Chatterjee, Y. Zhang, J. Zeng, N. R. Sahoo, and X. Luo, Phys. Rev. C **101**, 034902 (2020).
[30] X. Luo and N. Xu, Nucl. Sci. Tech. **28**, 112 (2017).
[31] X. Luo, J. Xu, B. Mohanty, and N. Xu, J. Phys. G **40**, 105104 (2013).
[32] See Supplemental Material at http://link.aps.org/supplemental/10.1103/9l69-2d7p for CBWC, effect of centrality resolution on cumulant ratios, and comparison of net proton C_4/C_2 data from BES-II vs BES-I and with various baselines.
[33] A. Bzdak and V. Koch, Phys. Rev. C **86**, 044904 (2012).
[34] M. Kitazawa and M. Asakawa, Phys. Rev. C **86**, 024904 (2012); **86**, 069902(E) (2012).
[35] X. Luo, Phys. Rev. C **91**, 034907 (2015); **94**, 059901(E) (2016).
[36] T. Nonaka, M. Kitazawa, and S. I. Esumi, Phys. Rev. C **95**, 064912 (2017); **103**, 029901(E) (2021).
[37] X. Luo and T. Nonaka, Phys. Rev. C **99**, 044917 (2019).
[38] R. Barlow, in *Proceedings of the Conference on Advanced Statistical Techniques in Particle Physics* (2002), pp. 134–144, arXiv:hep-ex/0207026.
[39] P. Braun-Munzinger, B. Friman, K. Redlich, A. Rustamov, and J. Stachel, Nucl. Phys. A **1008**, 122141 (2021).
[40] S. A. Bass *et al.*, Prog. Part. Nucl. Phys. **41**, 255 (1998).
[41] M. Bleicher *et al.*, J. Phys. G **25**, 1859 (1999).
[42] A. Bazavov *et al.*, Phys. Rev. D **101**, 074502 (2020).
[43] D. Bollweg, H. T. Ding, J. Goswami, F. Karsch, S. Mukherjee, P. Petreczky, and C. Schmidt, Phys. Rev. D **110**, 054519 (2024).
[44] X. An *et al.*, Nucl. Phys. A **1017**, 122343 (2022).
[45] L. Adamczyk *et al.* (STAR Collaboration), Phys. Rev. C **96**, 044904 (2017).
[46] STAR Collaboration, HEPData (collection), 10.17182/hepdata.159490 (2025).